The Astrophysical Journal, 619:L71–L74, 2005 January 20
© 2005. The American Astronomical Society. All rights reserved. Printed in U.S.A.

RECENT STAR FORMATION IN NEARBY GALAXIES FROM *GALAXY EVOLUTION EXPLORER* IMAGING: M101 AND M51

Luciana Bianchi,[1] David A. Thilker,[1] Denis Burgarella,[2] Peter G. Friedman,[3] Charles G. Hoopes,[1] Samuel Boissier,[4] Armando Gil de Paz,[4] Tom A. Barlow,[3] Yong-Ik Byun,[5] Jose Donas,[2] Karl Forster,[3] Timothy M. Heckman,[1] Patrick N. Jelinsky,[6] Young-Wook Lee,[5] Barry F. Madore,[4] Roger F. Malina,[2] D. Christopher Martin,[3] Bruno Milliard,[2] Patrick Morrissey,[3] Susan G. Neff,[7] R. Michael Rich,[8] David Schiminovich,[3] Oswald H. W. Siegmund,[6] Todd Small,[3] Alex S. Szalay,[1] Barry Y. Welsh,[6] and Ted K. Wyder[3]

Received 2004 April 15; accepted 2004 May 21; published 2005 January 17

ABSTRACT

The *Galaxy Evolution Explorer* (*GALEX*) Nearby Galaxies Survey is providing deep far-UV and near-UV imaging for a representative sample of galaxies in the local universe. We present early results for M51 and M101, from *GALEX* UV imaging and Sloan Digital Sky Survey optical data in five bands. The multiband photometry of compact stellar complexes in M101 is compared to population synthesis models, to derive ages, reddening, reddening-corrected luminosities, and current/initial masses. The *GALEX* UV photometry provides a complete census of young compact complexes on a ≈160 pc scale. A galactocentric gradient of the far-UV/near-UV color indicates younger stellar populations toward the outer parts of the galaxy disks, the effect being more pronounced in M101 than in M51.

Subject headings: galaxies: individual (M51, M101) — galaxies: star clusters — ultraviolet: galaxies

Online material: color figures

1. INTRODUCTION

The study of stellar cluster systems and compact associations provides us with insight into a galaxy's star formation history and stellar content. Far-UV (FUV) and near-UV (NUV) bands are a sensitive probe for detection of young stellar clusters and for measurement of their physical parameters and—combined with optical data—of their extinction (Bianchi et al. 1999; Chandar et al. 1999).

The *Galaxy Evolution Explorer* (*GALEX*) Nearby Galaxies Survey (NGS), described by Bianchi et al. (2005a, 2005b), is providing deep FUV and NUV imaging for a representative sample of ≈200 galaxies in the local universe. We present early *GALEX* NGS data of M101 and M51. We also use five-band optical imaging from the Sloan Digital Sky Survey (SDSS). We derive ages, reddening, and current/initial masses for the compact UV sources in M101 (§ 3). Radial profiles of UV brightness and color are presented in § 4.

The two galaxies studied in this Letter have been previously imaged in a broad FUV band ($\lambda_{\rm eff} \approx 1521$ Å) by the Ultraviolet Imaging Telescope (UIT). The UIT data were analyzed by Kuchinski et al. (2000), Waller et al. 1997 (M101), Hill et al. 1997 (M51), and Hoopes et al. (2001). While the UIT FUV images revealed morphological differences with respect to the optical bands and the brightest stellar complexes, the *GALEX* data yield significant advances. First, both FUV and NUV bands are available, providing an essentially reddening-free color that gives a direct indication of the age (for compact sources) independent of the extinction estimate, while the UV-to-optical wide baseline is very sensitive to both extinction and age (§ 3). Second, *GALEX*'s detectors afford greater sensitivity and linearity than the UIT data (which were recorded on film), measuring UV emission out to larger disk radii and down to fainter (by about 3 mag) fluxes (§ 4).

2. OBSERVATIONS AND DATA ANALYSIS

The *GALEX* instrument is described by Martin et al. (2005) and its on-orbit performance by Morrissey et al. (2005). *GALEX* FUV (1350–1750 Å) and NUV (1750–2750 Å) imaging was obtained with total exposure times of 1414 and 1041 s for M51 and M101. Assuming distances of 9.6 and 7.4 Mpc (M51: Sandage & Tammann 1974; M101: Kelson et al. 1996), the 4.″6 FWHM *GALEX* point-spread function (PSF) corresponds to 209 and 157 pc. The 1 σ (at the PSF scale) NUV (FUV) sensitivity limit of the *GALEX* images is 27.9 (27.8) AB mag arcsec^{-2} for M51 and 27.6 (27.5) AB mag arcsec^{-2} for M101.

We also used SDSS imaging of M51 and M101 in the *ugriz* filters. The resolution of the optical data (1″–2″, ≈70 and 50 pc for M51 and M101, respectively) is superior to that of *GALEX*, and in some cases the *GALEX* UV sources are resolved into two or three optical sources. The different angular resolutions were taken into account when matching the UV and optical sources. For the analysis in § 3, we focus on the smallest scale detections in each galaxy, thus sampling the star-forming complexes in M101 and M51 on a scale corresponding to the *GALEX* resolution. Postpipeline processing and photometry on the *GALEX* and SDSS images were performed using the SEx-

[1] Deptartment of Physics and Astronomy, Johns Hopkins University, 3400 North Charles Street, Baltimore, MD 21218; bianchi@pha.jhu.edu, dthilker@pha.jhu.edu, hoopes@pha.jhu.edu, heckman@pha.jhu.edu.

[2] Laboratoire d'Astrophysique de Marseille, BP8, Traverse du Siphon, 13376 Marseille Cedex 12, France; denis.burgarella@oamp.fr, roger.malina@oamp.fr, bruno.milliard@oamp.fr.

[3] California Institute of Technology, MC 405-47, 1200 East California Boulevard, Pasadena, CA 91125; friedman@srl.caltech.edu, tab@srl.caltech.edu, krl@srl.caltech.edu, cmartin@srl.caltech.edu, patrick@srl.caltech.edu, ds@srl.caltech.edu, tas@srl.caltech.edu, wyder@srl.caltech.edu.

[4] Observatories of the Carnegie Institution of Washington, 813 Santa Barbara Street, Pasadena, CA 91101; agpaz@ipac.caltech.edu, barry@ipac.caltech.edu.

[5] Center for Space Astrophysics, Yonsei University, Seodaemun-ku, Seoul 120-749, Korea; byun@obs.yonsei.ac.kr, ywlee@obs.yonsei.ac.kr.

[6] Space Sciences Laboratory, University of California at Berkeley, 601 Campbell Hall, Berkeley, CA 94720; patj@ssl.berkeley.edu, ossy@ssl.berkeley.edu, bwelsh@ssl.berkeley.edu.

[7] Laboratory for Astronomy and Solar Physics, NASA Goddard Space Flight Center, Greenbelt, MD 20771; neff@stars.gsfc.nasa.gov.

[8] Department of Physics and Astronomy, University of California at Los Angeles, Box 951547, Knudsen Hall, Los Angeles, CA 90095; rmr@astro.ucla.edu.

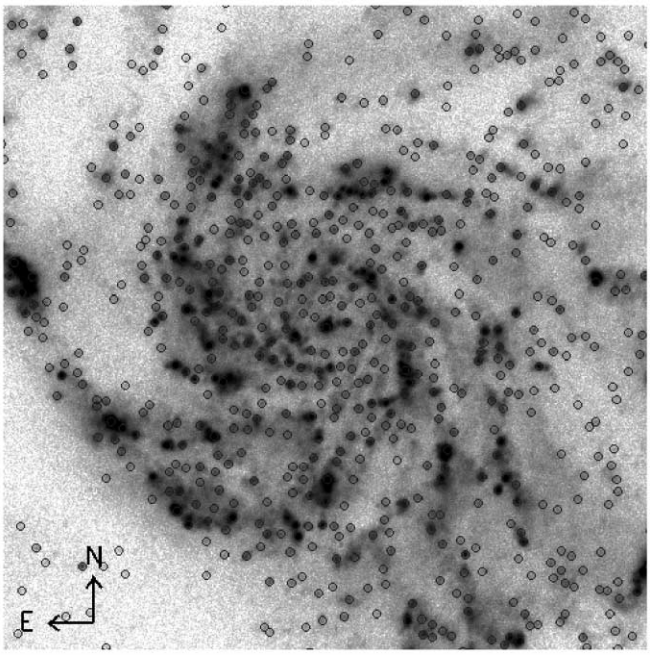

FIG. 1.—Portion (12.5 arcmin^2) of a *GALEX*-NUV image of M101. The compact UV sources with photometric errors less than 0.2 mag are indicated with circles.

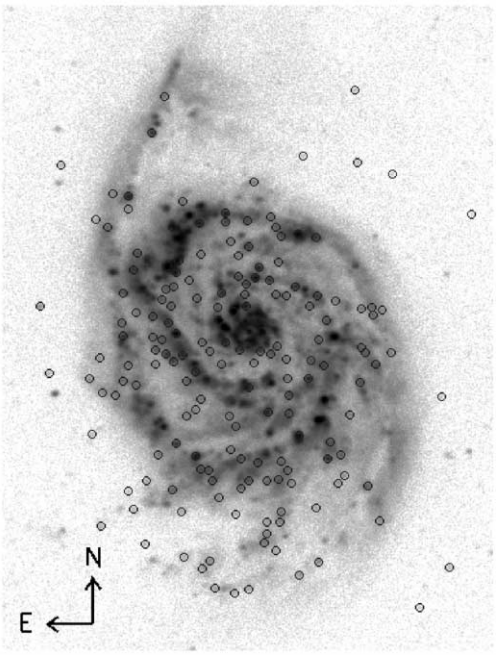

FIG. 2.—Same as Fig. 1, but for M51 (9′.5 × 12′.5).

tractor (Bertin & Arnouts 1996) and IRAF APPHOT packages. To obtain our master list of "pointlike" sources we first ran SExtractor on the NUV imagery after removal of the diffuse background, using a detection kernel matched to the *GALEX* NUV PSF (4″.6). The background was estimated using a circular median-filter of diameter 10″.5 (7 pixels). Such background removal is crucial in order to obtain a complete SExtractor catalog in bright regions of M51 and M101. We then passed this list of compact NUV sources to the APPHOT package, running PHOT (with recentering enabled) on background-subtracted versions of the *GALEX* FUV, NUV, and convolved SDSS images. Sources that shifted in position by more than 4″ in any band were eliminated. Finally, PHOT was used to measure fluxes for all surviving compact sources with 4″ aperture radius, and aperture corrections based on isolated field stars were applied. Figures 1 and 2 show the *GALEX* NUV image for the two galaxies. The matched sources with photometric errors better than 0.2 mag in the UV bands are shown. Table 1 gives the number of detected sources in each band.

The final matched catalog was based on the NUV source list (the deepest UV band) and includes only NUV sources having a counterpart in at least one other band. The photometry procedures were verified by comparing our results with both *GALEX* and SDSS pipeline photometry on portions of the same images outside the galaxy body, where the standard pipeline results are reliable. We found complete consistency within the errors. We applied our photometry technique in the regions containing the galaxies, where the standard *GALEX* and SDSS pipelines break down. We use the flux calibration from the *GALEX* Internal Release version 0.2.

3. THE PHYSICAL PARAMETERS OF THE COMPACT COMPLEXES

The measured colors for the compact UV sources in M101 were compared to synthetic colors computed from the Bruzual & Charlot (2003) models for integrated populations, for the cases

TABLE 1
THE SAMPLE OF SOURCES IN THE DIFFERENT BANDS

	Error < 0.2 mag		Error < 0.1 mag		Error < 0.05 mag	
Band	Sources	Magnitude Limit	Sources	Magnitude Limit	Sources	Magnitude Limit
			M101			
FUV	1034	22.1	383	20.8	82	19.1
NUV	2179	22.8	898	21.7	249	20.4
u	1351	22.4	878	21.7	389	20.6
g	1315	23.0	939	22.3	539	21.4
r	1233	22.6	851	22.0	467	21.2
i	1066	22.4	715	21.6	419	20.4
z	796	21.1	468	20.4	248	19.1
			M51			
FUV	200	22.5	78	21.1	25	19.6
NUV	622	22.9	257	21.9	83	20.7
u	268	...	140	21.8	54	20.7
g	253	...	153	22.5	76	21.6
r	228	...	131	21.9	71	21.0
i	205	...	115	21.7	65	20.6
z	170	...	85	20.2	42	19.3

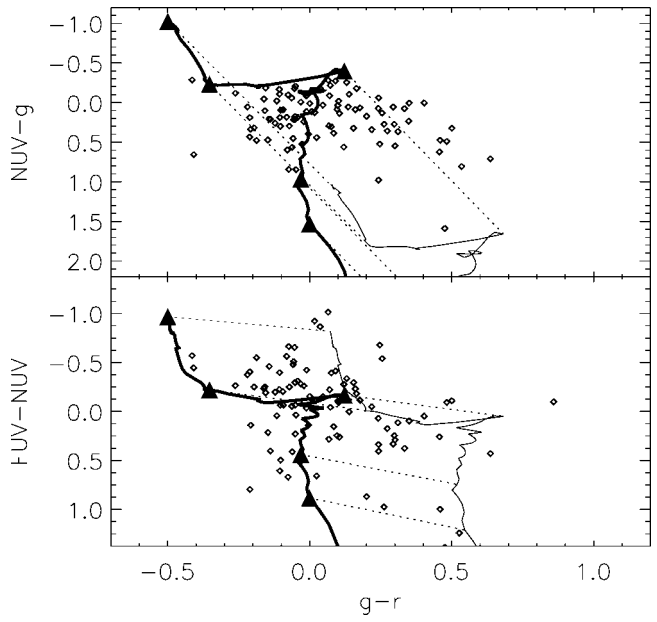

FIG. 3.—Color-color diagrams for the compact UV sources in M101. Only sources with photometric errors less than 0.1 mag (*GALEX* bands) and less than 0.05 mag (SDSS bands) are plotted. The solid black curve shows the intrinsic colors for SSP models as a function of age. Model colors reddened with $E(B-V) = 0.5$ are shown with a thin black line (dotted lines connect the intrinsic and reddened color for the same model at representative ages). Filled black triangles mark ages (in log years) of 6.0, 6.7, 6.9, 8.0, and 8.3. [*See the electronic edition of the Journal for a color version of this figure.*]

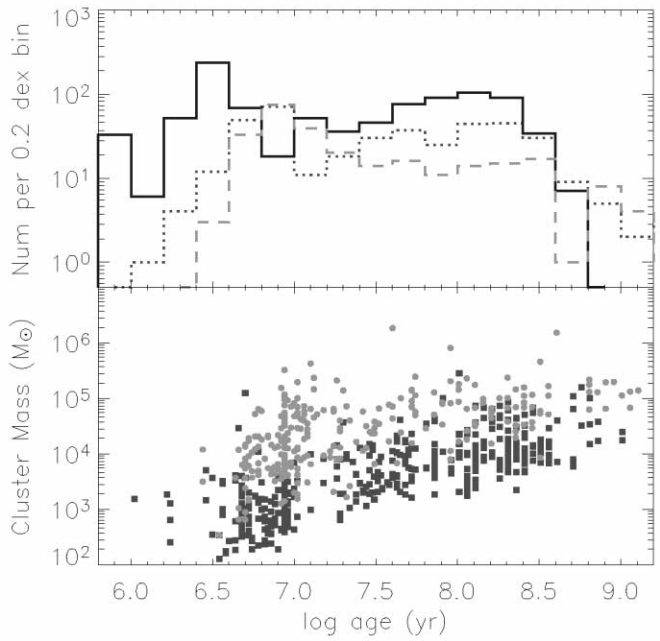

FIG. 4.—*Top*: Histogram of the derived ages for the compact stellar complexes in M101 from SED fits (*dashed green line*) and from FUV − NUV color only (*solid blue line*). Only sources with small photometric errors and good SED fits are included in the green sample, limiting the sample to about 300 sources. All sources with errors less than 0.2 mag in FUV and NUV bands are included in the blue (*solid*) histogram (about 1100 sources). The truncation at ages less than 10^9 yr for the blue histogram (FUV − NUV) is a selection effect of the sample. The sharp decline of the green histogram at older ages includes selection effects of the sample, as well as a possible effect of actual disruption. The dotted red histogram shows the cluster sample from one *HST* WFPC2 image (from R. Chandar et al. 2004, in preparation). *Bottom*: Masses vs. ages derived for our UV sources (*green circles*; parameters from SED fits) and for the cluster sample of R. Chandar et al. (2004, in preparation; *red squares*). [*See the electronic edition of the Journal for a color version of this figure.*]

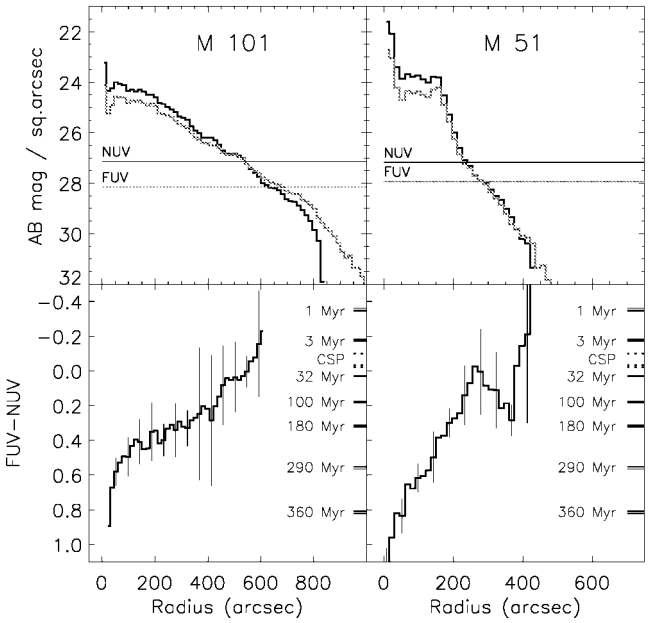

FIG. 5.—Radial profiles of FUV and NUV median surface brightness and FUV − NUV color. Errors ($\pm 1\ \sigma$) are shown for representative points of the FUV − NUV color. For the brightness profiles, errors range between 0.075 and 0.3 mag in the range 24–29 mag. The horizontal lines are the estimated sky surface brightness in each band. On the FUV − NUV panels, we show (*line segments*) theoretical FUV − NUV values for SSP models of ages 1, 3, 32, 100, 180, 290, and 360 Myr and CSP models of ages 0.1, 1, and 10 Gyr (*dashed segments*).

of single burst (simple stellar population [SSP]) and of continuous star formation (composite stellar population [CSP]), as a function of age. As expected (because we are sampling UV-bright compact complexes), most sources are better represented by an SSP spectral energy distribution (SED). We assume solar metallicity and a Chabrier (2003) initial mass function (mass range 0.1–100 $M_\odot$). Because the UV sources are mostly very young complexes, the analysis is not very sensitive to metallicity. For instance, the FUV − NUV color of an SSP model with solar metallicity for 1, 10, and 100 Myr is FUV − NUV = −0.35, −0.06, and 0.18 (in the AB mag system). The model colors for the same ages at $z = 0.008$ differ by ≤0.1, which leads to an uncertainty in the age by up to a factor of 3, and typically by ≤2, depending on the age. Kennicutt et al. (2003) show that solar metallicity is appropriate out to ≈6′, including the majority of our sources.

Figure 3 shows color-color diagrams of the sources compared to the models. We derived physical parameters by comparing the measured magnitudes to the model colors. Because the observed SEDs depend on the cluster age (intrinsic SED) and on the wavelength-dependent interstellar extinction, we reddened the model colors for different amounts of extinction and reddening types. Two different methods were used and the results compared. In the first method, we used the *GALEX* measurements alone and estimated the cluster ages by comparing the FUV − NUV color to the models. Reddening has a negligible effect on the FUV − NUV color, for $E(B-V)$ values associated with these galaxies. For instance, model colors for $E(B-V) = 0.2$ (MW-type extinction, $R_V = 3.1$) differ from the unreddened colors by ≤0.01, up to 100 Myr. Second, we fit all the measured multiband magnitudes with the synthetic colors to derive age and $E(B-V)$ concurrently, by χ^2 minimization, taking into account the photometric errors (L. Bianchi et al. 2004, in preparation).

Ages determined from the FUV − NUV color and by the

SED fit of the UV-to-optical bands, respectively, agree for most of the sources within the errors but are discrepant for some sources, where a color gradient may be present. We adopt the age from the SED fits, which represents the average over the area included in the aperture, for the sources with errors less than 0.05–0.10 mag (SDSS and *GALEX* bands, respectively). These ages are shown in the green-dashed histogram in Figure 4, and ages derived by the FUV − NUV color only (for the UV sources with FUV and NUV errors <0.2 mag) are shown by the blue (*solid*) histogram. This sample (about 1100 sources) includes a large number of (mostly younger) sources eliminated by the error cuts in the SED-fit sample. We note that individual errors in the ages derived by the FUV − NUV color in the range of log age (in years) = 6.5–7.5 may be larger than the bin size, as FUV − NUV does not vary appreciably in this range. For this reason, and for the selection effects limiting the sources with good SED fits, we do not attempt to interpret this histogram in terms of star formation history. We point out, however, the great sensitivity of the *GALEX* UV imaging to detect and measure the youngest sources. The sharp decline in the number of sources at older ages is due mostly to our magnitude limits and color selection effect. However, disruption may be more effective for these large-scale complexes than for bound clusters. Once reddening and age are determined for each complex, the reddening-corrected luminosity and age yield the current (and thus the initial) mass, by comparison with the same models (Fig. 4, *bottom panel*).

Figure 4 also shows the cluster sample detected in one *HST* WFPC2 field with *U*, *B*, *V*, and *I* measurements by R. Chandar et al. (2004, in preparation) in M101. Given the higher spatial resolution, the *HST* photometry samples bound stellar clusters, while our *GALEX* census samples the star-forming complexes on spatial scales of $\lesssim$160 pc. For M51 we do not perform a similar analysis given the smaller number of compact sources detected and distortion of the images, which limits the accuracy of compact sources photometry.

In summary, the *GALEX* images provided a complete census of young, compact star-forming complexes. The UV bands are extremely sensitive to young stellar populations; e.g., the (intrinsic) FUV − *r* (≈FUV − *V*) colors of clusters (SSP) with ages of 1, 10, and 100 Myr are −1.78, −0.30, 1.11 (AB mag), while the *u* − *g* (*g* − *r*) [approximately *B* − *V* (*U* − *B*)] colors are −0.49, 0.06, −0.03 (−0.39, 0.01, 0.69). Thus, by including *GALEX* measurements we gain a finer resolution for parameters of young associations and complexes, hence a clearer, unbiased census of recent star formation. Figure 4 indicates that star formation in M101 occured over the last 10^9 yr, both in stellar clusters (R. Chandar et al. 2004, in preparation) and in larger complexes (*GALEX* results; this Letter).

4. THE PROPERTIES OF THE STELLAR POPULATIONS

To explore the average properties of the stellar population as a function of galactocentric distance, we computed radial profiles of the FUV and NUV median surface brightness for each galaxy within concentric elliptical annuli, oriented in accordance with the galaxy inclination and position angle (M101: $i = 18°$, P.A. = 39°; Bosma et al. 1981; M51: $i = 20°$, P.A. = 170°; Rots et al. 1990). Within each annulus we measured the median surface brightness (thus removing the discrete peaked sources and the foreground stars) and subtracted an average sky background, determined in a wide elliptical annulus exterior to the galaxy. In Figure 5 we plot the surface brightness as a function of radius in the two *GALEX* bands, as well as the FUV − NUV color. Values of this color for SSP and CSP models are indicated for a range of ages. As shown previously, this color is essentially reddening-free, thus gives a direct indication of the age. Observed colors are redder than CSP models for a wide range of ages, across most of the galaxy, excluding this scenario. SSP models represent the extreme opposite of the CSP scenario, and SSP ages have only indicative value, since we are comparing colors of azimuthally averaged populations, and single bursts of star formation (clusters, associations) would likely be localized. The SSP ages indicate a more recent star formation activity toward outer regions (spanning 2 dex in age) for M101 and much less conspicuous fluctuations in M51, while the bulge has an older (average) age.

The comparison of Figure 5 with the FUV radial profile from UIT data (Kuchinski et al. 2000) shows the advantage of the *GALEX* measurements. In addition to providing the FUV − NUV color, for both M101 and M51 the profiles in Figure 5 extend to larger galactocentric radii, sampling outer disk areas, about 3 mag fainter than the UIT data (note again that we use AB magnitudes, which differ from the UIT magnitude system—for FUV—by ≈2.8 mag).

The radial profiles of the FUV − NUV color in the Local Group galaxies M33 and M31, and in M83 (Thilker et al. 2005a, 2005b), show the same trend of the FUV − NUV color becoming bluer outward, the magnitude of the color gradient differing from galaxy to galaxy. An extensive comparison among a representative sample of nearby galaxies will follow in a forthcoming paper.

GALEX is a NASA Small Explorer, launched in 2003 April. We gratefully acknowledge NASA's support for construction, operation, and science analysis of the *GALEX* mission, developed in cooperation with the Centre National d'Etudes Spatiales of France and the Korean Ministry of Science and Technology. We are very grateful to R. Chandar for helpful discussions and to the referee for many useful suggestions.

REFERENCES

Bertin, E., & Arnouts, S. 1996, A&AS, 117, 393
Bianchi, L., Chandar, R., & Ford, H. 1999, Mem. Soc. Astron. Italiana, 70, 629
Bianchi, L., Madore, B., Thilker, D., Gil de Paz, A., & Martin, C. 2004a, in The Local Group as an Astrophysical Laboratory, in press
Bianchi, L., et al. 2004b, BAAS, 203, 91.12
Bosma, A., Goss, W. M., & Allen, R. J. 1981, A&A, 93, 106
Bruzual, G., & Charlot, G. 2003, MNRAS, 344, 1000
Chabrier, G. 2003, PASP, 115, 763
Chandar, R., Bianchi, L., Ford, H., & Salasnich, B. 1999, PASP, 111, 794
Hill, J. K., et al. 1997, ApJ, 477, 673
Hoopes, C. G., Walterbos, R. A. M., & Bothun, G. D. 2001, ApJ, 559, 878
Kelson, D. D., et al. 1996, ApJ, 463, 26
Kennicutt, R. C., Jr., Bresolin, F., & Garnett, D. R. 2003, ApJ, 591, 801
Kuchinski, L. E., et al. 2000, ApJS, 131, 441
Martin, D. C., et al. 2005, ApJ, 619, L1
Morrissey, P., et al. 2005, ApJ, 619, L7
Rots, A. H., Crane, P. C., Bosma, A., Athanassoula, E., & van der Hulst, J. M. 1990, AJ, 100, 387
Sandage, A., & Tammann, G. A. 1974, ApJ, 194, 559
Thilker, D., et al. 2005a, ApJ, 619, L67
———. 2005b, ApJ, 619, L79
Waller, W. H., et al. 1997, ApJ, 481, 169